Figure S1

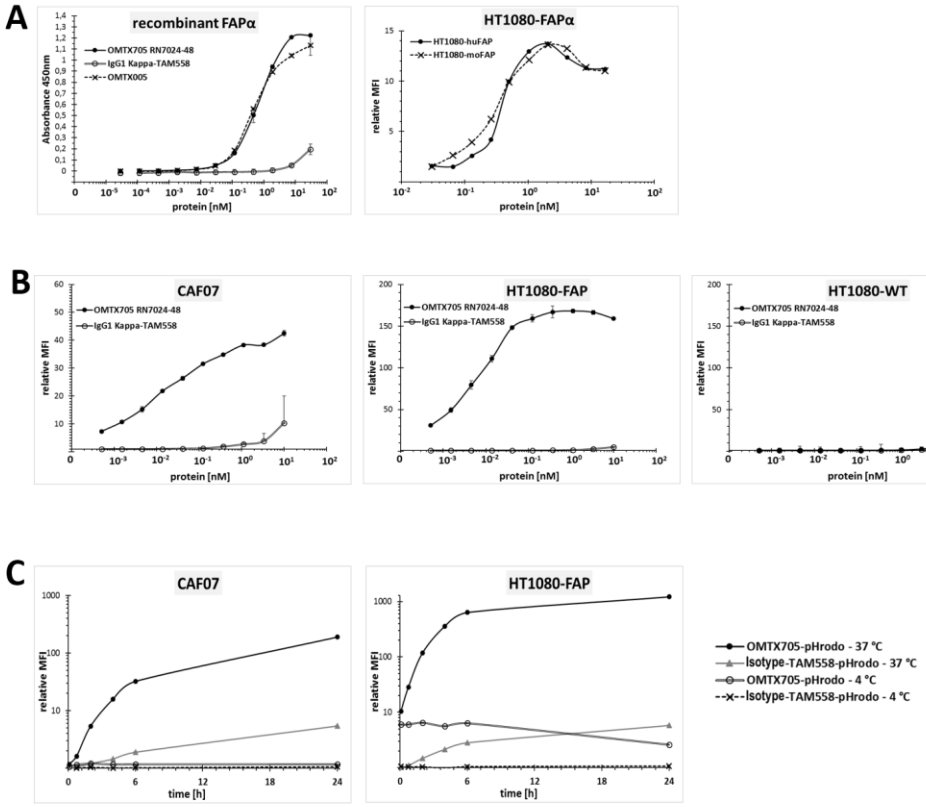

Figure S1. OMTX705 binding and internalization in HT1080-WT, -FAP and CAFs

A. Left graph: Binding of OMTX705 to immobilized human FAP recombinant protein determined by ELISA. Bound molecules were revealed with an HRP-anti-hu Fc secondary antibody. Right graph: Binding of OMTX005 anti-FAP antibody to human (HT1080-huFAP) versus murine (HT1080-moFAP) FAP-transfected cells measured by FACS analysis of PE-labeled anti-huFc secondary antibody. **B.** Binding of OMXTX705 to primary CAFs (CAF07), HT1080-FAP and HT1080-WT cells measured similarly by FACS. For binding studies (A, B), isotype IgG1-Kappa/TAM558 ADC and unconjugated OMTX005 anti-FAP antibody were used as negative and positive controls, respectively. **C.** FACS analysis of internalization of pHrodo-labeled OMTX705 and isotype IgG1-kappa/TAM558 ADC in primary CAFs (CAF07) and HT1080-FAP expressing cells. Compounds were incubated at 30nM with cells, either at 37ºC or 4ºC, for 5, 45, 120, 240, 360 min, and 24hrs. Cells were analyzed by FACS using PE channel.

Figure S2

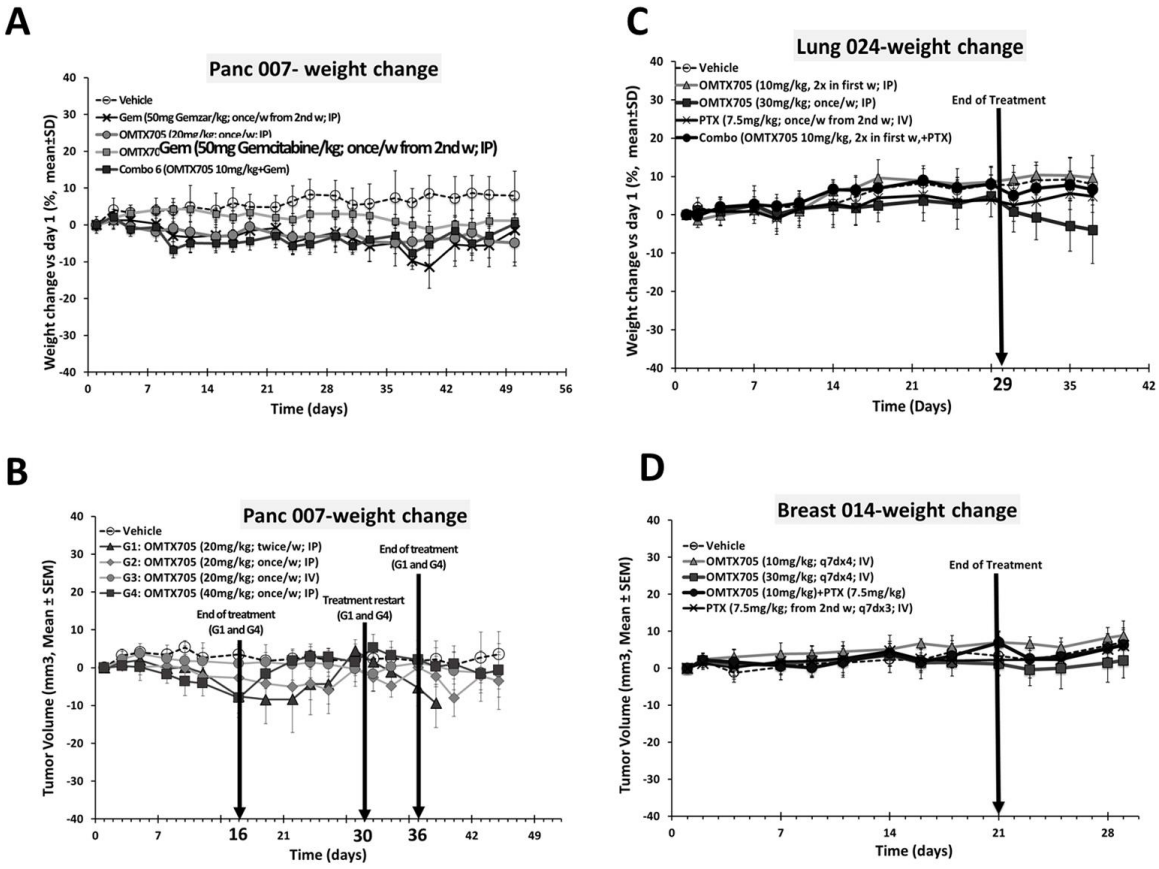

Figure S2. Weight change of mice bearing Panc 007, Lung 024 and Breast 014 tumors.

A. Mice bearing Panc 007 tumor were treated with OMTX705 and/or gemcitabine as indicated. **B.** Like A, except mice were treated with single agent OMTX705 either continuously or in cyclic intervals. **C.** Mice bearing Lung 024 tumor were treated with OMTX705 and/or paclitaxel as indicated. **D.** Mice bearing Breast 014 tumor were treated with OMTX705 and/or paclitaxel as indicated.

Figure S3

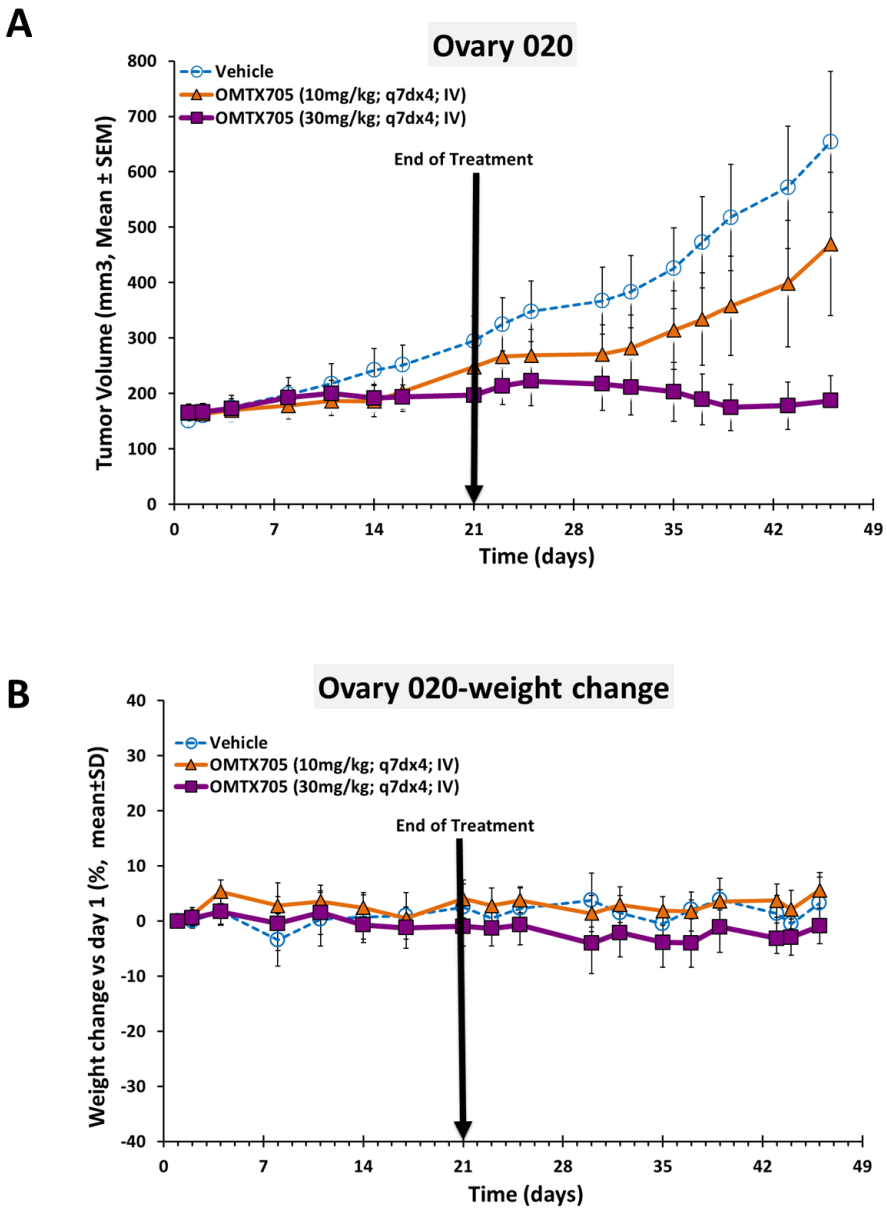

Figure S3. OMTX705 Activity in the Immunodeficient Patient Derived Xenografts (PDX) Models of Ovarian Cancer.

A. Activity of single agent OMTX705 in mice bearing Ovary 020 tumor models. Animals were treated with OMTX705 at indicated doses. **B.** Weight changes of mice bearing Ovary 020 tumor. OMTX705 was well-tolerated with no significant weight loss.

Figure S4

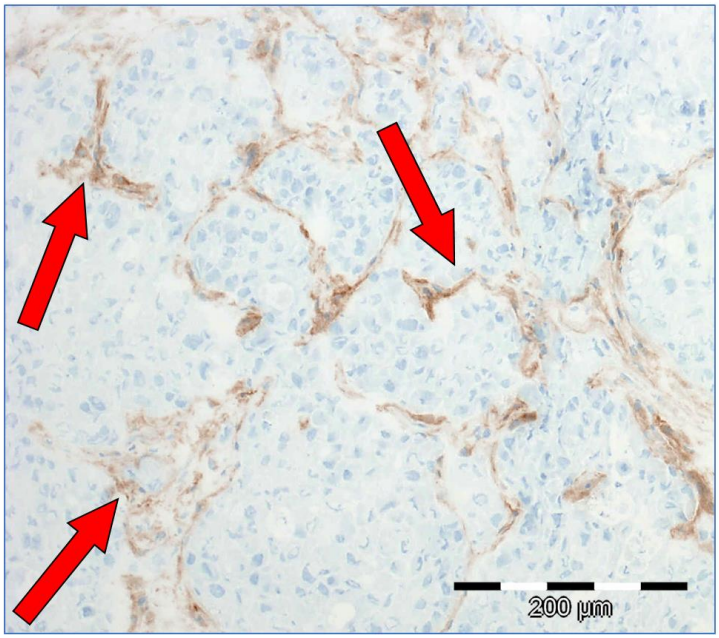

Figure S4. FAP expression in frozen tumor samples from humanized mice bearing CTG-0860 NSCLC PDX tumor. Immunostaining with OMTX005 anti-FAP antibody. Red arrows: FAP staining in fusiform stromal cells from tumor microenvironment.

Figure S5

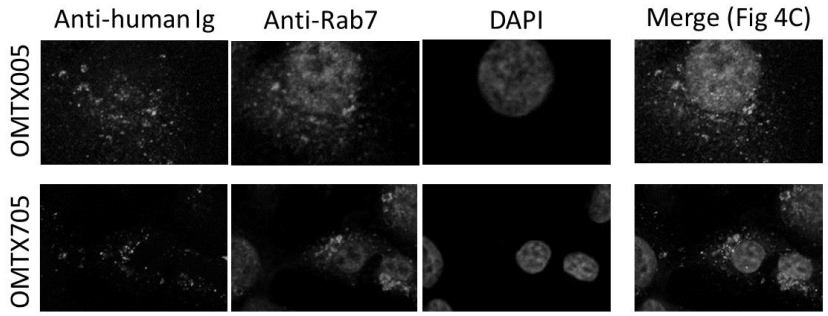

Figure S5. Immunofluorescence individual staining of OMTX005 or OMTX705 in HT1080-FAP cells analyzed by confocal microscopy.

Individual staining of OMTX005, OMTX705, rabbit anti-Rab-7, and nuclei, revealed with an FITC-labeled anti-human antibody, PE-labeled anti-rabbit antibody, and DAPI, respectively, with the corresponding merged image represented in Fig 4B. Black and white pictures.

Figure S6

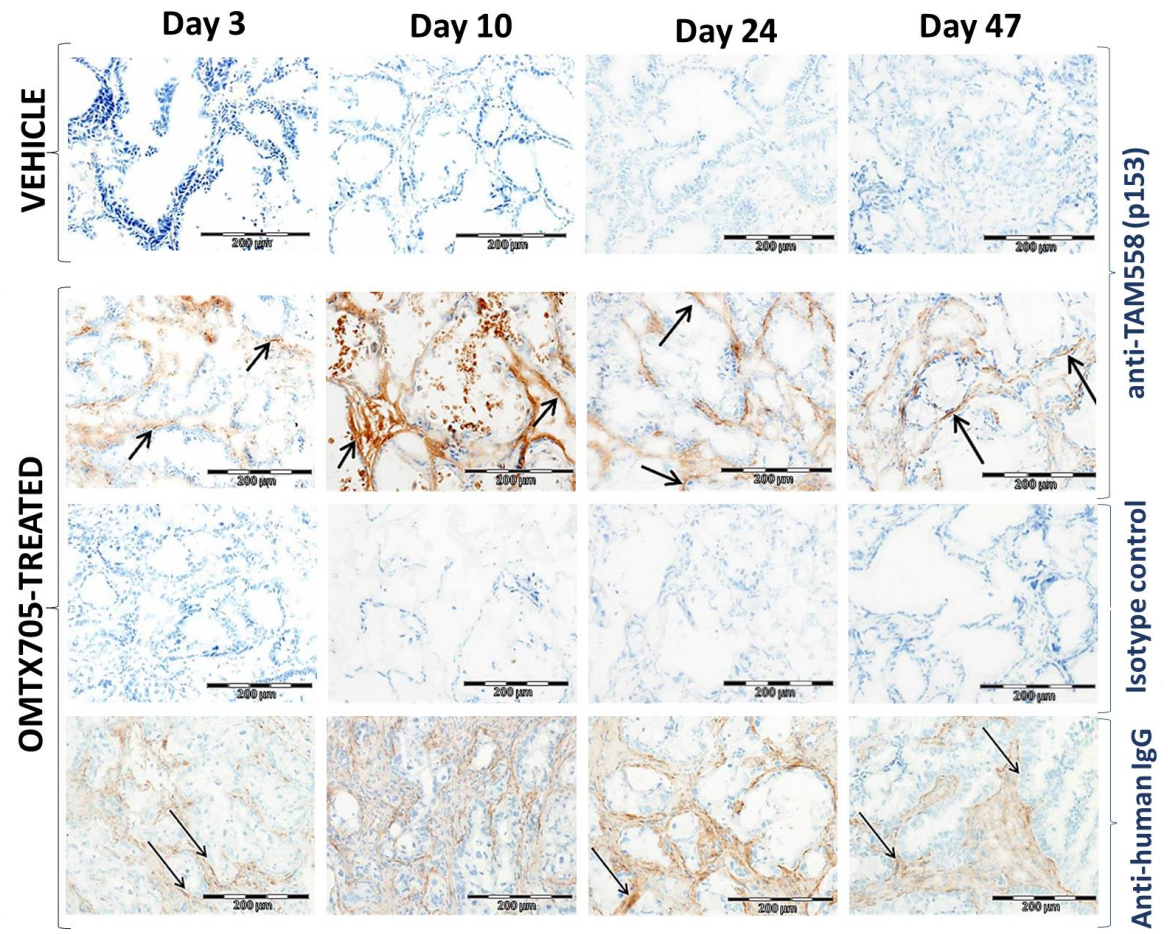

Figure S6. Analysis of payload versus OMTX705 distribution in tumors from Panc 007 model. Immunohistochemical staining of vehicle- versus OMTX705-treated tumor samples from Panc 007 PDX mice extracted at day 3, 10, 24, and 47 after treatment started. Staining with rabbit anti-TAM558 payload p153 pAb, rabbit isotype control antibody, and anti-human IgG antibody, showed that positive staining was obtained with rabbit anti-TAM558 p153 antibody but not with isotype antibody in OMTX705-treated tumors. No staining was observed with anti-TAM558 p153 antibody in vehicle-treated tumors indicating the specific detection of TAM558 payload in OMTX705-treated tumor samples when using p153 antibody. Black arrows: Payload or OMTX705 staining in fusiform stromal cells from tumor microenvironment.

Figure S7

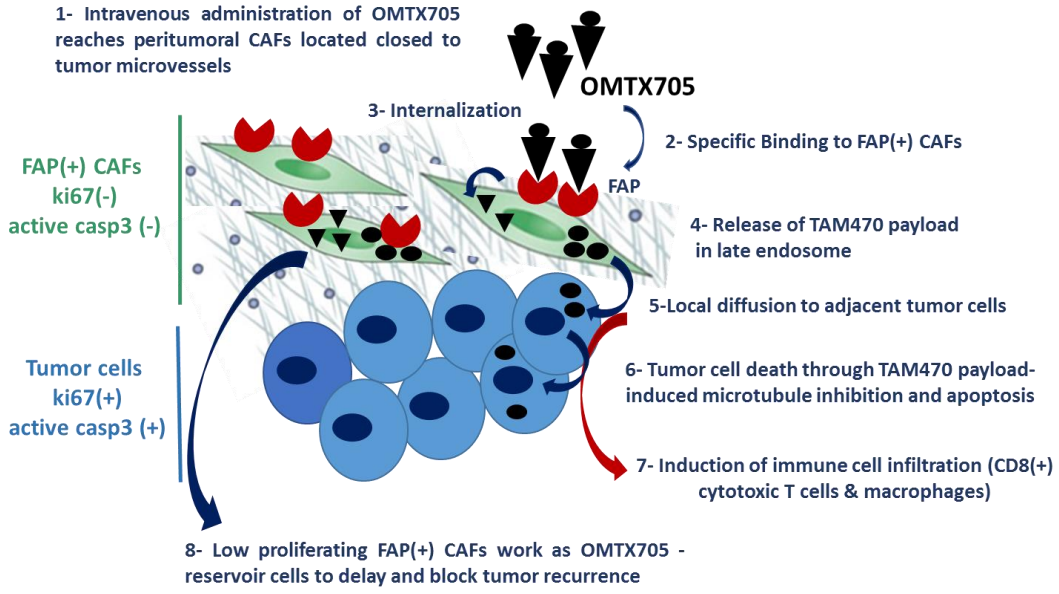

Figure S7. Schematic summary of findings and proposed mechanism of action of OMTX705.